



**Manchester
Metropolitan
University**

Noguchi, HK, Kaur, S, Krettli, LM, Singla, P, McClements, J, Snyder, H, Crapnell, RD ORCID logoORCID: <https://orcid.org/0000-0002-8701-3933>, Banks, CE ORCID logoORCID: <https://orcid.org/0000-0002-0756-9764>, Novakovic, K, Kaur, I, Gruber, J, Dawson, JA and Peeters, M (2022) Rapid electrochemical detection of levodopa using polyaniline-modified screen-printed electrodes for the improved management of Parkinson's disease. *Physics in Medicine*, 14. p. 100052. ISSN 2352-4510

Downloaded from: <https://e-space.mmu.ac.uk/631374/>

Version: Published Version

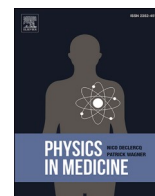
Publisher: Elsevier

DOI: <https://doi.org/10.1016/j.phmed.2022.100052>

Usage rights: Creative Commons: Attribution-Noncommercial-No Derivative Works 4.0

Please cite the published version

<https://e-space.mmu.ac.uk>



Rapid electrochemical detection of levodopa using polyaniline-modified screen-printed electrodes for the improved management of Parkinson's disease

Henrique K. Noguchi^{a,1}, Sarbjeet Kaur^{b,c,1}, Luiza M. Krettli^d, Pankaj Singla^b, Jake McClements^b, Helena Snyder^e, Robert D. Crapnell^f, Craig E. Banks^f, Katarina Novakovic^b, Inderpreet Kaur^c, Jonas Gruber^g, James A. Dawson^h, Marloes Peeters^{b,*}

^a Faculdade de Ciências Farmacêuticas, Universidade de São Paulo, Av. Prof. Lineu Prestes, 580, São Paulo, SP, CEP 05508-000, Brazil

^b Newcastle University, School of Engineering, Merz Court, Claremont Road, Newcastle Upon Tyne, NE1 7RU, UK

^c Department of Chemistry, Centre for Advanced Studies, Guru Nanak Dev University, Amritsar, Punjab, 143005, India

^d Departamento de Engenharia Química, Escola Politécnica, Universidade de São Paulo, Avenida Prof. Luciano Gualberto, trav. 3, 380, São Paulo, SP, CEP 05508-900, Brazil

^e University of Virginia, School of Engineering and Applied Science, 351 McCormick Rd, Charlottesville, VA, 22904, USA

^f Manchester Metropolitan University, Faculty of Science and Engineering, John Dalton Building, Chester Street, Manchester, M1 5GD, UK

^g Departamento de Química Fundamental, Instituto de Química, Universidade de São Paulo, Av. Prof. Lineu Prestes, 748, São Paulo, SP, CEP 05508-000, Brazil

^h Chemistry – School of Natural and Environmental Sciences, Newcastle University, Newcastle upon Tyne, NE1 7RU, UK

ARTICLE INFO

Keywords:

Biosensors
Levodopa
Parkinson's disease
Electrochemical testing
Polymer chemistry
Screen-printed electrodes

ABSTRACT

A portable test to rapidly determine levels of levodopa, the drug used to treat Parkinson's disease, can improve clinical management of the disease. In this study, screen-printed electrodes (SPEs) were modified with polymers to facilitate the electrochemical detection of levodopa. Cyclic voltammetry was used to deposit a thin layer of polyaniline on the electrode surface. Scanning electron microscopy revealed high surface coverage, which did not impact the electrode's conductivity. Differential pulse voltammetry measurements with the polyaniline-modified electrodes enabled the measurement of levodopa at physiologically relevant concentrations with discrimination between a common interferent (ascorbic acid) and a structurally similar compound (L-tyrosine). However, the use of the polymer layer did not permit differentiation between levodopa and dopamine; the only difference in these molecules is that levodopa has an amino acid moiety whereas dopamine has a free amine group. Density functional theory calculations demonstrated that aniline formed a hydrogen bond between the amino group of the monomer and the *meta*-hydroxyl group, which is present in both levodopa and dopamine, with similar binding energies (-53.36 vs -50.08 kJ mol⁻¹). Thus, the polymer-functionalised SPEs are a valuable tool to measure compounds important in Parkinson's disease, but further refinement is needed to achieve selective detection.

1. Introduction

Parkinson's disease (PD) is an incurable and progressive neurological disorder which is rapidly growing in prevalence [1]. The most effective treatment to control bradykinetic symptoms that are apparent in PD involves treatment with levodopa (L-dopa), a precursor to dopamine. However, this drug has limited efficacy and a short half-life, meaning most patients require a complex drug regime with multiple L-dopa doses

over a 24-h period [2,3]. Moreover, the dosage is highly dependent on diet, gender, lifestyle and stage of disease [4]. During the time intervals when medication is working, referred to as "on periods", patients experience significant improvement of PD symptoms. Furthermore, low levels of medication lead to "off periods" where there is loss of critical functions such as speech and mobility whereas high medication levels can result in debilitating dyskinesias [5]. The current method to physically assess the disease and prescribe treatment by neurologists involve

* Corresponding author. Newcastle University, School of Engineering, Merz Court, Newcastle upon Tyne, NE1 7RU, UK.

E-mail address: Marloes.peeters@newcastle.ac.uk (M. Peeters).

¹ H. K. Noguchi and S. Kaur share first authorship since they have contributed equally to the work.

clinical evaluation (typically six-monthly) and use of the MDS-Unified Parkinson's Disease Rating Scale (MDS-UPDRS) [6]. These laborious PD assessment scales necessitate multiple in-person visits, which has been complicated during the COVID-19 pandemic and led to significant worsening of physical activity and mental health of PD patients [7]. Real-time information on L-dopa and dopamine levels offers an objective manner to guide clinical management of PD, including decisions on medication dosage. Furthermore, abnormal levels of dopamine play a role in several other neurological disorders such as depression [8] and schizophrenia [9].

The concentration of L-dopa in plasma of patients with PD is generally between 5 and 20 μM depending on medication levels [10]. It is possible to measure L-dopa levels in serum with chromatographic techniques, but they require a lab environment for analysis and have long turn-around times [11]. Thus, it is necessary to move towards point-of-care devices that can measure L-dopa levels in a fast (minutes) and low-cost manner. Electrochemical biosensing for clinical biomarker analysis has received particular attention recently due to the rapid, low-cost, and portable nature of the measurement technique, with an estimated growth in publications of >200% in the last fifteen years [12]. Both L-dopa and dopamine are electroactive and therefore there is no need for a redox probe to facilitate electrochemical detection. However, direct electrochemical sensing is complicated since there is an abundance of interferents in bodily fluids (e.g., ascorbic acid, uric acid) that exhibit overlapping electrochemical signals [13]. The structure of dopamine and L-dopa, including that of the precursor L-tyrosine and ascorbic acid, a common interferent, are shown in Scheme 1.

Selective receptors, such as enzymes [14] or molecularly imprinted polymers (MIPs) [15] have shown promise for detection of L-dopa in buffered solutions or artificial solutions that mimic clinical samples. Synthetic receptors such as MIPs can also be applied to dopamine sensing, with an overview of strategies presented in Ref. [16]. Interference of ascorbic acid can be avoided through surface modification with overoxidised polypyrrole in combination with nanomaterials [17]. Another method involves the use of a system comprised of vanadium-substituted polyoxometalates, copper oxide and chitosan-palladium, which was able to selectively detect DA with a limit

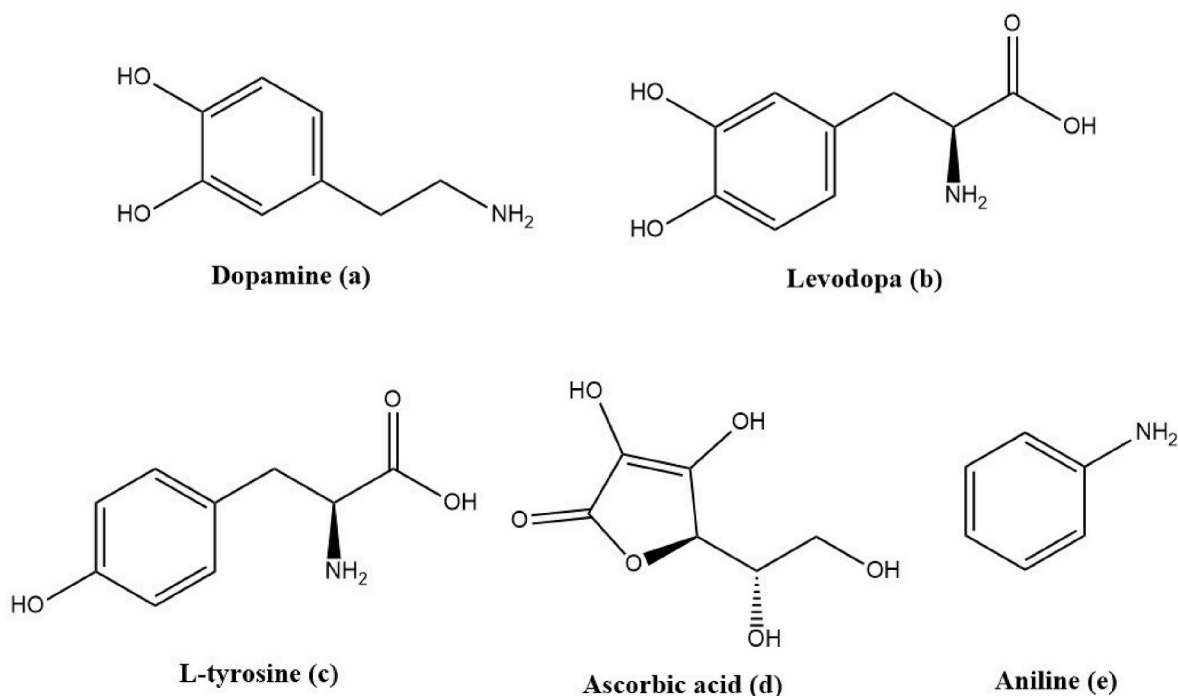
of detection (LoD) as low as 45 pM [18]. Hannah et al., [19] have shown that thin-film electrodes can accurately detect dopamine between concentrations of 50 pM - 1 mM without requiring the aforementioned surface modifications.

In this manuscript, we will focus on SPEs which have several advantages over traditional electrodes including low-cost, high reproducibility, and simple fabrication and cleaning procedures [20,21]. It was shown that polymer particles can be directly embedded into screen-printing ink to facilitate detection of a range of biomarkers and neurotransmitters, including dopamine [22,23]. However, drawbacks of this strategy include long preparation time (at least one week to extract and synthesize particles), sparse surface coverage leading to low sensitivity, and not being able to conduct electrochemical measurements since the polymer material is insulating. We report a simple method to modify electrodes with polymer material to enable detection of L-dopa. Computational modelling is employed to screen a range of monomers, since evaluating the interactions between functional monomers and the target molecule is an accurate predictor for the affinity of the polymer and analyte of interest [24]. Subsequently, the monomers with the highest binding affinity are functionalised onto SPEs using electrodeposition and lithographic methods. It is shown that polyaniline (PANI) can discriminate between L-dopa and dopamine and similar amino acids (e.g., L-tyrosine) and other components abundant in bodily fluids (e.g., ascorbic acid). By optimising measurements conditions (buffer, pH) and the electrochemical detection technique, we can measure L-dopa and dopamine concentrations at physiologically relevant concentration. This research paves the way towards a simple and low-cost method of monitoring PD medication levels, thus leading to better clinical management.

2. Experimental section

2.1. Reagents

L-dopa (Pharmaceutical Secondary Standard), hydrochloric acid (37% in water), pyrrole (reagent grade 98%), methacrylic acid (99%, containing 250 ppm hydroquinone monomethyl ether as inhibitor),



Scheme 1. The structures of dopamine (a), L-dopa (b) in addition to L-tyrosine (c) and ascorbic acid (d) that were used to analyse the selectivity. Aniline (e) was the functional monomer that was used to prepare polyaniline-modified electrodes that promoted binding to the surface.

aniline (>99.5%), phenol (99%), L-tyrosine, ascorbic acid, potassium ferrocyanide K₄[Fe(CN)₆] and potassium ferricyanide K₃[Fe(CN)₆], potassium chloride and sodium chloride (>99.5%) were purchased from Sigma Aldrich (Gillingham, UK). Dopamine hydrochloride was obtained from Acros Organics (Geel, Belgium). Citric acid (>99%) was acquired from Alfa Aesar (Haverhill, MA, USA). Sodium citrate dihydrate (>99%) was obtained from Fisher Scientific (Loughborough, UK). Sodium citrate/acetate buffered solutions (0.1 M) were prepared with deionized (DI) water with resistivity <18.2 M cm. Graphite SPEs (3.1 mm) were prepared according to Ref. [25], which involved screen-printing a graphite ink formulation (Gwent Electronic Materials Ltd) onto a standard polyester substrate. Subsequently, curing was performed at 60 °C for 30 min with a dielectric material from Gwent Electronic Materials Ltd. (Monmouthshire, UK) to define the rectangular shape of the SPE for easy handling.

2.2. Determination of optimum electrochemical sensing conditions

Electrochemical measurements were performed on a PalmSens4 potentiostat (PalmSens, Houten, the Netherlands) with an Ag/AgCl reference electrode and a Pt wire as counter electrode (Alvatek Ltd., Romsey, UK). L-dopa is unstable in solution and its concentration gradually diminishes after 48 h when it is kept at room temperature. Thus, it was ensured that fresh L-dopa solutions were prepared for each measurement [26]. Furthermore, the electrochemical response and solubility of L-dopa is strongly dependent on the buffer and pH. Therefore, the first cyclic voltammetry (CV) experiments (from 0 to +1.0 V, scan rate of 50 mV/s, concentration between 0 and 1 mM) were performed with blank SPEs to determine the optimal sensing conditions for L-dopa and dopamine. The pH was varied between 3 and 7 and sodium citrate and sodium acetate (0.1 M) buffered solutions were studied. The results for L-dopa were validated with UV-vis spectroscopy measurements with a Jenway 7205 UV-vis spectrophotometer (Stone, UK), analysing the peak of the analyte at 280 nm. UV-vis measurements were not performed for dopamine since, contrary to L-dopa, this molecule has high water solubility. Once the optimal electrochemical measurement conditions were determined, the influence of surface modification of the SPEs was studied. CV measurements for the polymer-modified electrodes were conducted in the range -0.4 V to +1.2 V since the presence of the polymer changes binding kinetics, which has an impact on the peak position, and therefore warrants evaluation of a wider potential window.

2.3. Functionalization and characterisation of polymer modified SPEs

Aniline was electrodeposited onto SPEs via chronoamperometry (CA) and cyclic voltammetry (CV). CA involved keeping a solution of aniline (3 mM), KCl (100 mM), and hydrochloric acid (10 mM) in water at a potential of +0.98V for several minutes. Electrodes were prepared fresh prior to each measurement due to the limited stability of polyaniline. CV measurements were conducted by cycling the same solution from -0.2 to +1.0 V with a scan rate of 0.5V/s. The best results were obtained with five cycles, but ten and fifteen cycles were also attempted. Furthermore, a portable Polytec (Karlsbad, Germany) UV light source (A = 365 nm) was used to functionalise aniline, acrylamide, methacrylic acid, and pyrrole onto the surface of SPEs.

After surface modification of the SPEs, immobilisation of the polymer was confirmed via conducting CV and electrochemical impedance spectroscopy (EIS) measurements of the polymer in a solution containing K₄[Fe(CN)₆] and K₃[Fe(CN)₆] (1 mM) and KCl (100 mM). The surface of the best performing electrodes was investigated with scanning electron microscopy (SEM) analysis with a Supra 40VP Field Emission (Carl Zeiss Ltd., Cambridge, UK) machine.

2.4. Electrochemical L-dopa measurements with polymer-modified SPEs

Subsequently, the prepared polymer-modified SPEs were studied with cyclic voltammetry and differential pulse voltammetry (DPV). DPV was initially conducted from 0 to 1.2 V, with a potential step of 0.04 V, pulse of 0.05 V, pulse time of 0.01 s and scan rate of 0.06 V/s according to a previously reported procedure [27]. DPV was subsequently conducted in the potential range from -0.4 V to +1.2 V.

Solutions were studied with concentration (0–1 mM) of dopamine and L-dopa in sodium citrate and sodium acetate buffered solutions, with and without the addition of K₄[Fe(CN)₆] and K₃[Fe(CN)₆] at 1 mM concentration and 100 mM of KCl as an electrolyte. The optimal measurement protocol was defined as the method which resulted in the highest current of the oxidation peak. The capability of the electrodes to selectively determine L-dopa and dopamine was evaluated by performing DPV measurements on mixed solutions with a 1:1 ratio of target with L-tyrosine and ascorbic acid at a concentration of 1 mM. In the case of L-tyrosine, a mixture of K₄[Fe(CN)₆] and K₃[Fe(CN)₆] was added to the solution but this was omitted for ascorbic acid measurements since the chemicals react with each other.

2.5. Density functionality theory (DFT) calculations

All calculations in this study were carried out using density functional theory (DFT) with the Vienna ab initio simulation package (VASP) [28]. Plane wave cut off energies of 520 eV were utilised for the geometry optimisation calculations. The projector augmented wave method [29] and the PBE exchange-correlation functional [30] were employed for all calculations. The Grimme DFT-D3 dispersion correction was also utilised to account for van der Waals interactions [31]. A k-point mesh spacing smaller than 0.05 Å⁻¹ was used for the geometry optimisation calculations.

Before calculating the binding energies between the monomer (aniline) and template molecules, the structure of each individual molecule was optimized. To reflect the preparation of a MIP, complexes between the functional monomer and template molecules were then established. A wide variety of possible binding sites and configurations were considered and simulated for each complex. The magnitude of the binding energy between the molecules in such a complex provides a quantitative indication of the driving force for its formation and stability. The binding energy (ΔE_b) was calculated using:

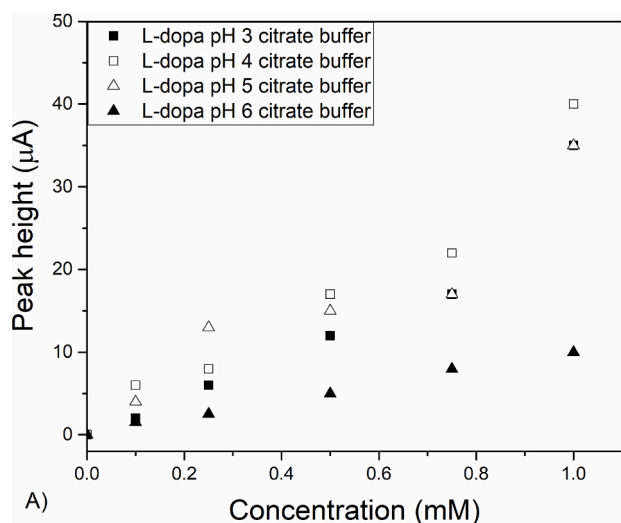
$$\Delta E_b = E_{\text{complex}} - E_{\text{aniline}} - E_{\text{template}} \quad (1)$$

where E_{complex} is the energy of a monomer-template complex, E_{aniline} is the energy of an aniline molecule and E_{template} is the energy of a template molecule. The more negative the ΔE_b value, the more stable the complex structure, and thus the higher predicted binding affinity.

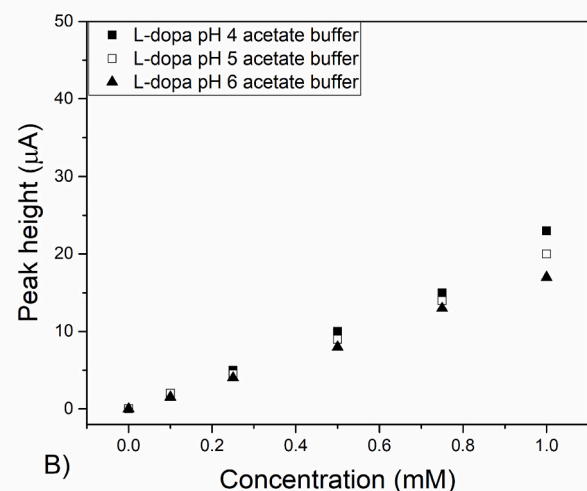
3. Results and discussion

3.1. Influence of pH and buffer on electrochemical measurements

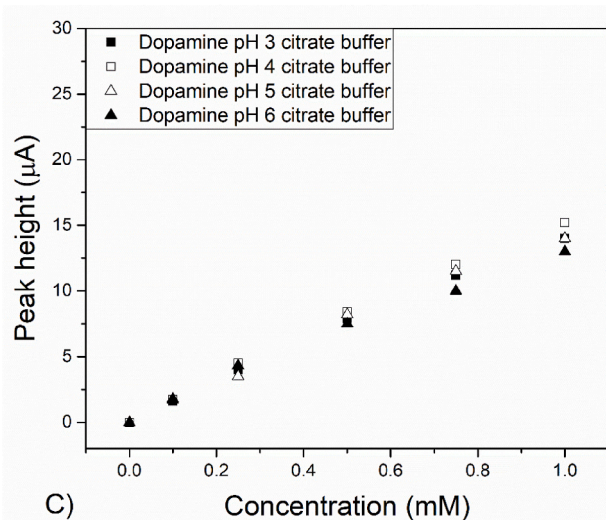
The optimal conditions of the buffer were investigated via analysing the response of buffered solutions spiked with known L-dopa and dopamine concentrations for CV measurements. Fig. 1 shows the measured calibration curves of L-dopa in citrate buffer (A), and L-dopa in acetate buffer (B), and of dopamine in citrate buffer (C) in pH range 3–6. The current at the maximum peak height was plotted versus the concentration. For L-dopa, at pH 3 the maximum peak height was around +0.52 V, whereas this gradually shifted to +0.50 V for pH 4 and 5, and +0.48 V for pH 6, respectively. For dopamine, the maximum peak height was +0.50 V at pH 3, +0.45 V at pH 4, +0.37 V at pH 5, and +0.32 V at pH 6. The degradation of L-dopa was observed at neutral and basic pH levels (the solution changed colour), which is why the electrochemical response at neutral and basic pH was not shown. Typical CV plots for L-



A)



B)



C)

Fig. 1. A) Electrochemical response of blank SPEs exposed to L-dopa concentrations in citrate buffer from pH 3–6 (A), acetate buffer from pH 4–6 (B), and exposed to dopamine in citrate buffer from pH 3–6 (C).

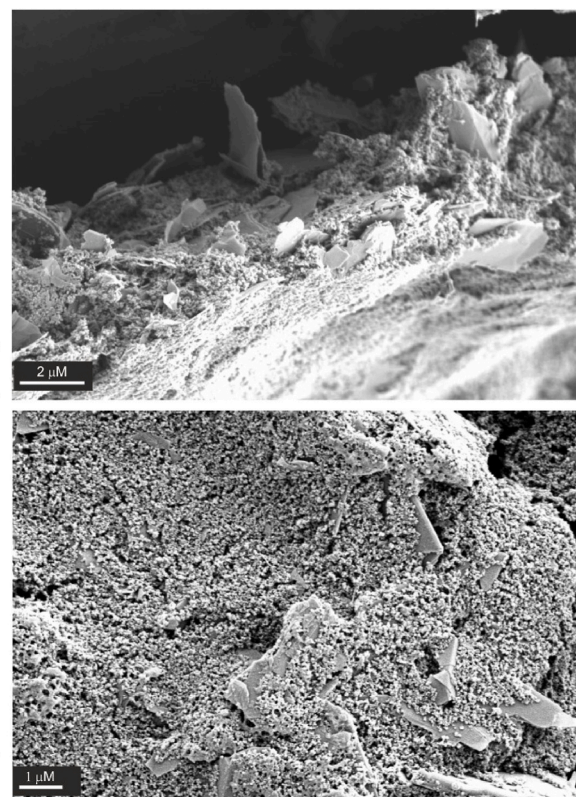


Fig. 2. SEM analysis of a blank SPE where graphite flakes are clearly visible (A). After oxidation of aniline on the SPE, the surface is covered with polymer material (B).

dopa and dopamine on blank SPEs are displayed in Figure S-1. Tables S-1 provides the relevant fit parameters for data shown in Fig. 1A, B and C.

L-dopa has limited solubility in water and therefore sodium citrate and acetate buffers are typically used for measurements. From Fig. 1, a higher electrochemical response was recorded when measuring in citrate buffer compared to acetate buffer. For instance, at $c = 1$ mM at pH 4 a peak height of ~ 37 μA was observed in citrate buffer whereas this was only ~ 25 μA in acetate buffer. We estimated the LoD with the three-sigma method, using the standard deviation on the analyte peak on three individual measurements. This led to an estimated LoD of 0.01 mM in citrate buffer (pH 4) and 0.1 mM in acetate buffer (pH 4).

Furthermore, the results were validated with spectroscopic measurements (Tables S-2), which indicated a higher response of the UV-vis signal in citrate buffer with optimal results achieved at pH 4. Thus, it was decided to conduct further experiments with dopamine in citrate buffer. Fig. 1c shows a clear linear trend of the dopamine oxidation peak with increasing concentration of L-dopa in citrate buffer, with an estimated LoD of 0.02 mM for the blank SPE at pH 4. The electrochemical response was similar in the pH range 4–5 for L-dopa, with a slightly slower response at pH = 3 but a significant lower current at pH = 6. It is known that the rate constant for intramolecular cyclization reactions of L-dopa and dopamine vary depending on the pH, which underlines why it is required to study this prior to the actual sensing experiments. However, no significant difference between pH 4–6 was observed for dopamine, albeit detection was limited in the neutral and alkali range.

To discriminate between L-dopa and dopamine and other common interferents such as L-tyrosine and ascorbic acid which have oxidation peaks in the same range, it is necessary to modify the electrode surface with charged polymers. The charges on the polymer surface are also pH dependent, which is why this is a crucial parameter to consider for sensing purposes.

3.2. Characterisation of functionalised electrodes

SPEs were modified with a range of polymer materials. Methacrylic acid and acrylamide were deposited onto the surface via free radical polymerisation initiated with UV-light. It was shown that the presence of the polymer significantly affected the conductivity of the SPEs (even in the case of a thin layer) as no significant response to a standard $K_4[Fe(CN)_6]/K_3[Fe(CN)_6]$ ($c = 1$ mM) redox couple could be detected. The focus was then directed towards conductive materials polypyrrole and PANI, polymers which have nitrogen-based heterocycles in the backbone. Aniline has a pKa value of 4.6, at which there was an equilibrium between positively charged aniline and its neutral form [32]. Since measurements were performed at pH 4, this facilitated formation of a hydrogen bond with the OH groups present in dopamine and L-dopa.

The conductivity of the surface architecture of the polymer-modified SPEs was analysed using a suite of complimentary characterisation techniques such as CV, EIS and scanning electron microscopy (SEM). CV in $K_4[Fe(CN)_6]/K_3[Fe(CN)_6]$ solution ($c = 1$ mM) revealed the influence of the polymer deposition on the conductivity of the electrode material; for sensing, it is necessary to work with conductive materials. Changes in the EIS spectra reflected the formation of an additional layer on the electrode surface.

SPEs were modified with pyrrole; however, the presence of the polymer on the surface led to a decrease in the electrochemical sensing of L-dopa compared to the blank electrode. Therefore, it was decided to further pursue aniline which has better electrochemical properties. SPEs were modified with aniline by keeping the potential fixed at +0.98 V for 100, 500, and 1000 s. The green colour on the SPEs clearly indicates that PANI was formed onto the electrode surface, with increasing colour intensity indicating that a thicker layer is formed over time (Figure S-2). EIS measurement showed high resistance on the surface, which is not desirable for sensing. When CA was run, polymer was constantly formed since the mixture is kept at oxidation potential. In contrast, when CV was performed, the polymer was only formed when the voltage was above the oxidation potential of the monomer. Therefore, CA is generally more

used to form dense layers whereas CV leads to patch-type polymer structures on the SPEs [33]. Thus, it was decided to move towards CV to deposit PANI, where the surface structure of respectively, 5, 10 and 15 different cycles was studied. It was found that the highest conductivity occurred after 5 cycles were performed; after more cycles, the response to the $K_4[Fe(CN)_6]/K_3[Fe(CN)_6]$ (1mM) redox couple was slowly decreasing. SEM analysis (Fig. 2) confirmed there was high coverage of PANI on the SPE but there was still unfunctionalized surface remaining after five cycles, indicating why this is beneficial for sensing of both L-dopa and dopamine. Analysis of the surfaces where more than five cycles were used to deposit PANI showed irregular coverage and the formation of multiple layers rather than the monolayer observed after five cycles. It is well-known that dopamine needs access to the surface to oxidize and therefore the signal is strongly dependent on the available surface area [34].

3.3. Computational modelling studies

DFT calculations were carried out to elucidate the binding mechanisms between the most promising functional monomer (aniline) and template molecules. The optimized lowest-energy configurations of the monomer-template complexes are given in Fig. 3. The binding mechanism for the aniline...L-dopa/dopamine complexes was the same and was dominated by the formation of a hydrogen bond between the amino group of aniline and the *meta*-hydroxyl group of L-dopa/dopamine. The binding energies of -53.36 and -50.08 kJ mol $^{-1}$ and hydrogen bond distances of 1.872 and 1.850 Å for the aniline...L-dopa/dopamine complexes, respectively, are very similar, illustrating the challenge of discriminating between these two template molecules. Potential binding between the amino groups of aniline and L-dopa/dopamine was also considered but the binding energies were significantly lower (35.70 and 39.56 kJ mol $^{-1}$, respectively).

Given that an excess of the aniline monomer was used to selectively discriminate between L-dopa and dopamine in our experiments, the possibility of two aniline monomers binding to L-dopa and dopamine

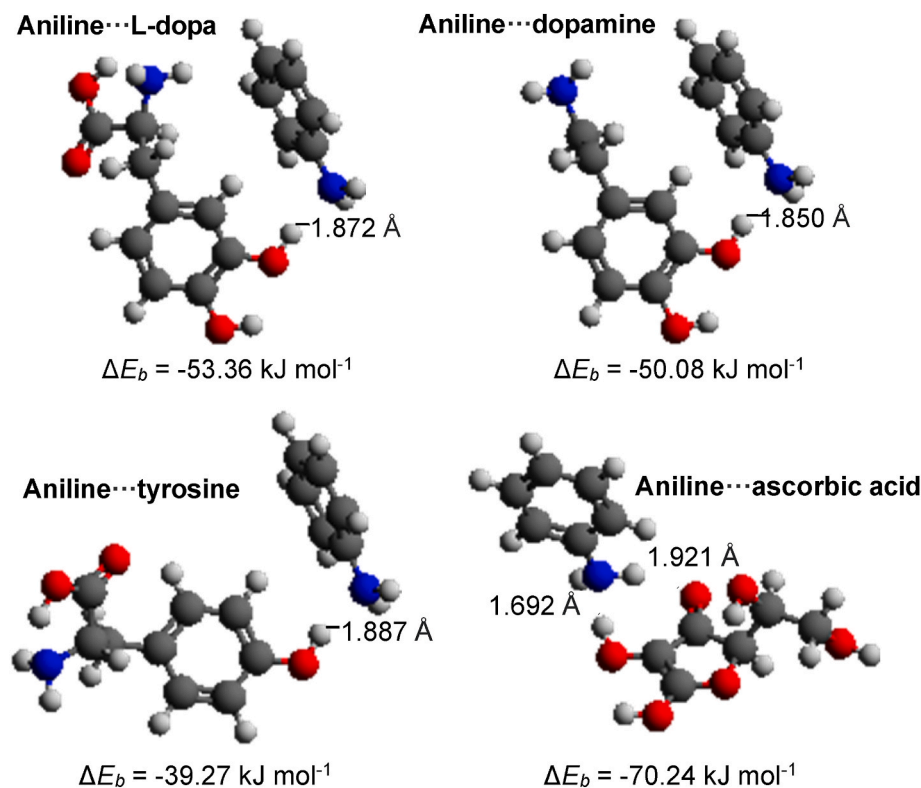


Fig. 3. Optimized geometries and binding energies for aniline...template molecule complexes. Intermolecular hydrogen bonds are indicated by the dashed lines.

was also considered. Figure S-3 shows the optimized lowest-energy configurations of the aniline...L-dopa/dopamine complexes with two aniline monomers. Binding via hydrogen bond formation between the amino group of aniline and the hydroxyl groups of L-dopa/dopamine was again favoured with strong binding energies of -85.87 and -78.44 kJ mol^{-1} , respectively, which illustrate the energetic benefit of forming aniline...L-dopa/dopamine complexes with two aniline monomers.

In addition to L-dopa/dopamine, the binding between the aniline monomer and potential interferents, namely, L-tyrosine, which possesses

a very similar molecular structure to L-dopa/dopamine, and ascorbic acid, which is abundant in bodily fluids, was also simulated. Fig. 3 shows that aniline binds with tyrosine via a similar mechanism to its binding with L-dopa and dopamine, namely, through hydrogen bond formation between the amino group of aniline and the hydroxyl group of tyrosine. However, the key difference is that aniline can only bind to tyrosine at the *para* position unlike its binding with L-dopa/dopamine, which preferentially occurs at the *meta*-hydroxyl group. Furthermore, the binding energy of -39.27 kJ mol^{-1} between aniline and tyrosine was smaller compared to the values obtained between aniline and L-dopa/

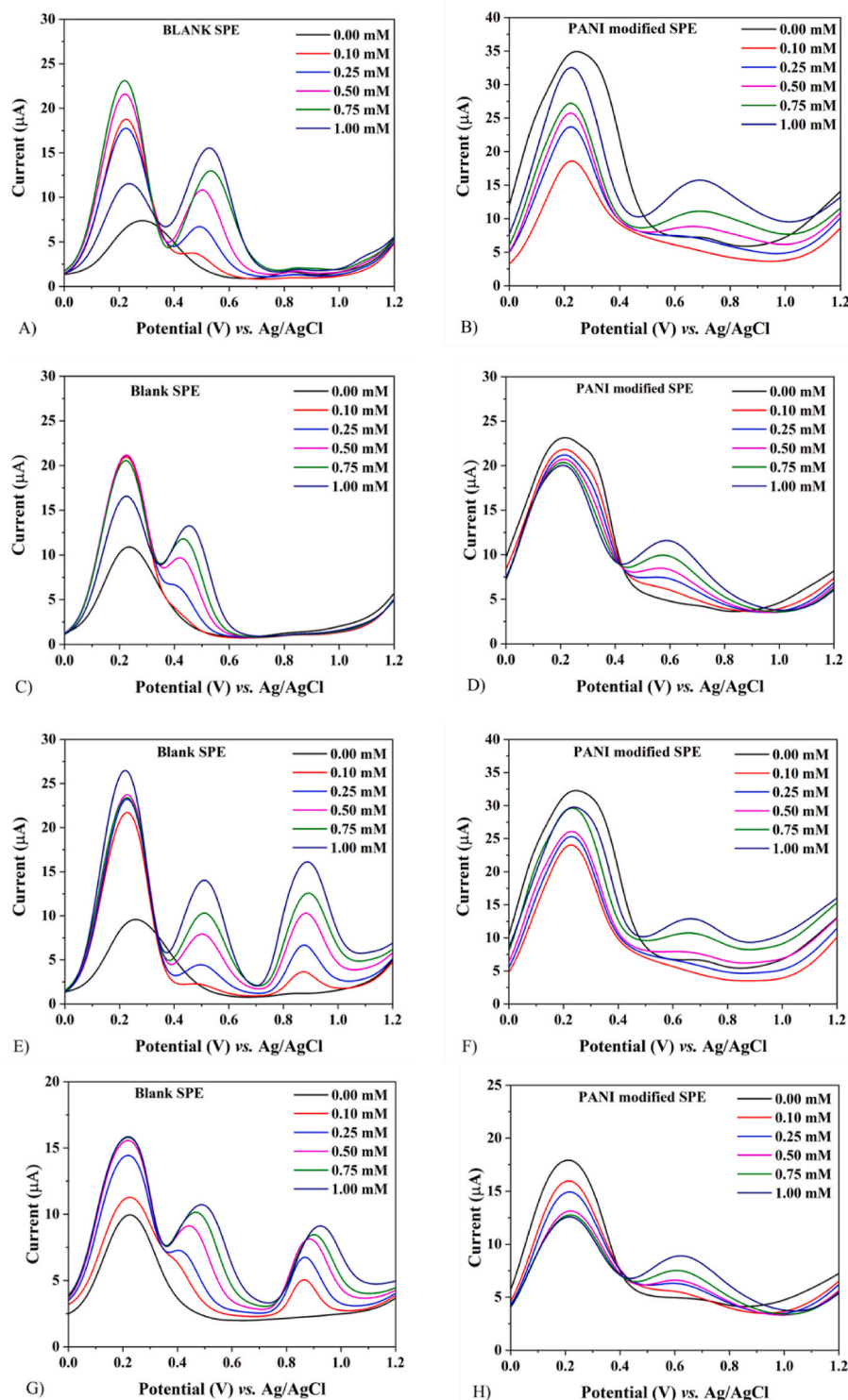


Fig. 4. Current vs potential for a blank SPE (A) and polyaniline-modified SPE (B) exposed to increasing concentrations of L-dopa. The response of a blank SPE (C) and polyaniline-modified SPE (D) to increasing concentrations of dopamine. In panel (E) the response of a blank SPE to a 1:1 mixture of L-dopa and tyrosine is presented, demonstrating the blank SPE is not capable of discriminating between the two compounds, which is the case for the polyaniline-modified SPE (F). A similar trend was observed for a 1:1 mixture of dopamine and tyrosine using a blank SPE (G) and polyaniline-modified SPE (H).

dopamine. These results explain why it was possible to discriminate between L-dopa/dopamine and tyrosine in our electrochemical experiments. In the case of ascorbic acid, the preferential binding sites for aniline are found to be the carbonyl oxygen and the adjacent hydroxyl group. Although the formed hydrogen bonds result in a large binding energy of $-70.24 \text{ kJ mol}^{-1}$, its unique binding mechanism means it was still possible to differentiate between this known interferent and the L-dopa target molecule.

3.4. Electrochemical measurements of polyaniline-modified SPEs

All these measurements were conducted in citrate buffer of pH 4 since this showed the highest electrochemical response towards both L-dopa and dopamine. DPV was used for sensing as it generally has higher sensitivity compared to CV. A wide potential window (-0.4 V to $+1.2 \text{ V}$) was selected since there are reports that peak separation between different catecholamines, including L-dopa and dopamine, can be achieved below pH 5 at negative voltage due to different kinetics of intramolecular cyclization rates [35,36]. Fig. 4 shows the electrochemical response for the blank and PANI-modified SPEs towards L-dopa and dopamine spiked solutions and mixtures of L-dopa or dopamine with L-tyrosine in a ratio 1:1.

First, it was clear that the electrochemical response (current) of both L-dopa and dopamine was not dependent on the presence of polyaniline on the surface. There was a significant shift in the position of the oxidation peak of the compounds of interest; this shifted from $+0.52 \text{ V}$ to $+0.68 \text{ V}$ for L-dopa, and from $+0.48 \text{ V}$ to $+0.59 \text{ V}$ for dopamine. This was not unusual since the presence of polyaniline will likely slow the electrochemical rate constant and lead to broader peaks shifting to the right of the spectrum. There was also a slightly higher background current, which was expected since conductive polymers can hold more charge than graphite itself and add variability to the surface structure. The LoD was not significantly impacted by the presence of the polymer on the electrode, meaning it was possible to detect L-dopa at plasma concentration levels relevant to PD patients [10]. For both the blank and polymer-modified SPEs, there was a clear response towards both L-tyrosine and ascorbic acid (Figure S-4). The polymer-modified did not show a response towards L-tyrosine and, in the case of ascorbic acid, the oxidation peak did not shift and therefore fell in the same region as PANI. When evaluating a 1:1 mixture of L-dopa and dopamine with L-tyrosine, the precursor of catecholamines, and ascorbic acid, a compound which is abundant in bodily fluids, significant difference between the blank SPE and polymer-modified SPE were observed. Without the presence of the polymer, the peaks of the interferents were clearly visible in the DPV plots for L-tyrosine (Figure S-4) with overlapping signals for ascorbic acid and L-dopa/dopamine (Figure S-4). Therefore, it was confirmed that the presence of the polymer was crucial to improve selective binding with no peaks of L-tyrosine or ascorbic acid seen when the electrodes were modified (Figure S-4). The computational modelling demonstrated that hydrogen bonds can be formed between the amino group of aniline and the *meta*-hydroxyl group of L-dopa/dopamine, meaning there was preferential binding of these compounds to the surface over L-tyrosine and ascorbic acid. As a result, it was possible to separate between L-dopa/dopamine and L-tyrosine and ascorbic acid, despite these compounds being similar in chemical functionality and/or size. Fig. 5 compares the peak current for the blank SPE and aniline-modified SPE for the target itself and when exposed to a mixture of the target with L-tyrosine. The relevant fit data is provided in Tables S-3.

Fig. 5 clearly demonstrates there is no significant change in current between blank SPEs and those modified with polyaniline. Thus, there was also no significant difference in sensitivity between the electrodes. However, the presence of the polymer enables discrimination between certain compounds, although it was not possible to distinguish between L-dopa and dopamine since the functional monomer interacts at the same position. Achieving peak separation was attempted by optimising

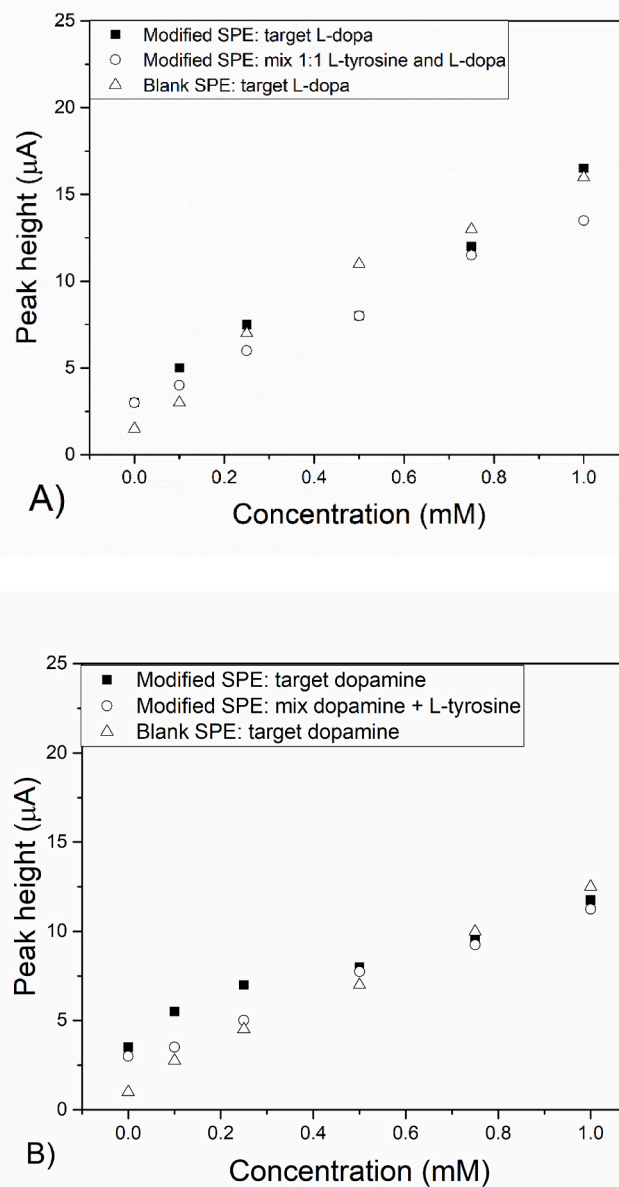


Fig. 5. The peak current for blank and modified SPEs when exposed to increasing concentration of L-dopa and L-dopa mixed with L-tyrosine (A) and for the blank and modified SPEs when exposed to increasing concentrations of dopamine and dopamine mixed with L-tyrosine (B).

the pH and evaluating the peak at -0.076 V . However, as this peak was substantially lower compared to the peak at $\sim 0.5 \text{ V}$, this did not enable detection at physiologically relevant levels as the sensitivity was reduced by at least two orders of magnitude. Previous studies [35,36] achieved a similar LoD as our sensor and compared this to existing electrochemical sensing platforms. These reports showed that it was possible to measure signals at -0.076 V to discriminate between different catecholamines using glassy carbon electrodes; however, the LoD was negatively impacted since the signal at negative voltage was considerably lower compared to the electrochemical peak at positive voltage. Moreover, glassy carbon electrodes are expensive and not suitable for point-of-care sensing unlike the low-cost and disposable SPEs employed in this study. SPEs offer higher commercial potential and are better suited towards continuous monitoring purposes. In the future, a mixture of monomers might be employed to improve selectivity of the modified SPEs and move the platform closer towards real life

applications. This is complicated to achieve with electrodeposition since different monomers have different optimal polymerisation conditions. Moreover, sample preparation needs to be considered since blood has a pH = 7.4 whereas this research showed that acidic conditions are beneficial for sensing. Thus, it could be that sample preparation will involve dilution with an appropriate buffer to enhance the electrochemical signal and ensure stability of L-dopa.

4. Conclusion

We developed a novel, straightforward sensor for the electrochemical detection of L-dopa using PANI-modified SPEs. Oxidation of aniline with hydrochloride acid was used to develop functionalised SPEs, with SEM demonstrating high coverage of the polymer on the electrode surface. With this straightforward and low-cost platform, it was possible to measure L-dopa and dopamine in the low mM range using DPV and discriminate between the structurally similar L-tyrosine and common interferent ascorbic acid due to hydrogen bond interactions between polyaniline and target compounds. However, it was not possible to discriminate between L-dopa and dopamine, which share a similar catechol structure and both possess a *meta*-hydroxyl group. This was in line with DFT results, which demonstrated that the binding mechanism for the aniline ...L-dopa/dopamine complexes was the same, with binding energies of -53.36 and -50.08 kJ mol⁻¹ and hydrogen bond distances of 1.872 and 1.850 Å, respectively, illustrating the challenge of discriminating between these two template molecules. This platform therefore has high potential for monitoring compounds that are important for management of PD, but further refinement of the monomer composition is needed to achieve selective sensing.

Author contributions

All authors have given approval to the final version of the manuscript.

Notes

The authors declare no competing financial interest.

Declaration of competing interest

The authors declare that they have no known competing financial interests or personal relationships that could have appeared to influence the work reported in this paper.

Data availability

Data will be made available on request.

Acknowledgements

JAD gratefully acknowledges Newcastle University for funding through a Newcastle Academic Track (NUAct) Fellowship. SK, IK and MP acknowledge the Commonwealth Commission for providing a Splitsite Scholarship to SK and for providing a grant to carry out the research. MP and JMC acknowledge support via an EPSRC Impact Accelerator Account.

We are thankful for the stimulating discussions with Prof Damion Corrigan to advice on the optimisation of the electrochemical sensing.

Appendix A. Supplementary data

Supplementary data to this article can be found online at <https://doi.org/10.1016/j.phmed.2022.100052>.

References

- [1] T. Pringsheim, N. Jette, A. Frolkis, T.D.L. Steeves, The prevalence of Parkinson's disease: a systematic review and meta-analysis, *Mov. Disord.* 29 (2014) 1583–1590, <https://doi.org/10.1002/mds.25945>.
- [2] W. Poewe, A. Antonini, J.C.M. Zijlman, P.R. Burkhardt, F. Vingerhoets, Levodopa in the treatment of Parkinson's disease: an old drug still going strong, *Clin. Interv. Aging* 5 (2010) 229–238, <https://doi.org/10.2147/CIA.S6456>.
- [3] R.A. Hauser, Levodopa: past, present, and future, *Eur. Neurol.* 62 (2009) 1–8, <https://doi.org/10.1159/000215875>.
- [4] J. Jankovic, L.G. Aguilar, Current approaches to the treatment of Parkinson's disease, *Neuropsychiatric Dis. Treat.* 4 (2008) 743–757, <https://doi.org/10.2147/NDT.S2006>.
- [5] A.S. Schrag, N. Quinn, Dyskinesias and motor fluctuations in Parkinson's disease: a community-based study, *Brain* 123 (2000) 2297–2305, <https://doi.org/10.1093/brain/123.11.2297>.
- [6] P. Martínez-Martín, C. Rodríguez-Blázquez, M. Alvarez, T. Arakaki, C. Arillo, P. Chaná, W. Fernández, N. Garretto, J.C. Martínez-Castrillo, M. Rodríguez-Violante, M. Serrano-Dueñas, D. Ballesteros, J.M. Rojo-Abuín, K.R. Chaudhuri, K. Merello, Parkinson's disease severity levels and MDS-Unified Parkinson's disease Rating Scale, *Park. Relat. Disord.* 21 (2015) 50–54, <https://doi.org/10.1016/j.parkrel.2014.10.026>.
- [7] A. Shalash, T. Roushdy, M. Essam, M. Fathy, N.L. Dawood, E.M. Abushady, H. Elrassas, A. Helmi, E. Hamid, Mental health, physical activity, and quality of life in Parkinson's disease during COVID-19 pandemic, *Mov. Disord.* 35 (2020) 1097–1099, <https://doi.org/10.1002/mds.28134>.
- [8] K.M. Tye, J.J. Mirzabekov, M.R. Warden, E.A. Ferenczi, H.-C. Tsai, J. Finkelstein, S.-Y. Kim, A. Adhikari, K.R. Thompson, A.S. Andalman, L.A. Gunaydin, I.B. Witten, K. Deisseroth, Dopamine neurons modulate neural encoding and expression of depression-related behaviour, *Nature* 493 (2013) 537–541, <https://doi.org/10.1038/nature11740>.
- [9] R. Brisch, S. Arthur, W. Rainer, B. Hendrik, H.-G. Bernstein, J. Steiner, B. Bogerts, K. Braun, Z. Jankowski, J. Kumaratilake, M. Henneberg, T. Gos, The role of dopamine in dopamine from a neurobiological and evolutionary perspective: old fashioned, but still in vogue, *Front. Psychiatr.* 5 (2014), <https://doi.org/10.3389/fpsy.2014.00047>.
- [10] J. Zhang, F. Qu, A. Nakatsuka, T. Nomura, M. Nagai, M. Nomoto, Pharmacokinetics of L-dopa in plasma and extracellular fluid of striatum in common marmosets, *Brain Res.* 54 (2003), <https://doi.org/10.1016/j.brainres.2003.08.065>.
- [11] M. Karimi, J.L. Carl, S. Loftin, J.S. Perlmutter, Modified high-performance liquid chromatography with electrochemical detection method for plasma measurement of levodopa, 3-O-methyldopa, dopamine, carbidopa, and 3,4-dihydroxyphenyl acetic acid, *J. Chromatogr. B* 836 (2006) 120–123, <https://doi.org/10.1016/j.jchromb.2006.03.027>.
- [12] R.D. Crapnell, N.C. Dempsey-Hibbert, M. Peeters, A. Tridente, C.E. Banks, Molecularly imprinted polymer based electrochemical biosensors: overcoming the challenges of detecting vital biomarkers and speeding up diagnosis, *Talanta Open* 2 (2020), 100018, <https://doi.org/10.1016/j.talo.2020.100018>.
- [13] K. Jackowska, P. Kryszinski, New trends in electrochemical sensing of dopamine, *Bioanal. Anal. Chem.* 405 (2012) 3753–3771, <https://doi.org/10.1007/s00216-012-6578-2>.
- [14] K.Y. Goud, C. Moonla, R.K. Mishra, C. Yu, R. Narayan, I. Litvan, J. Wang, Wearable electrochemical microneedle sensor for continuous monitoring of levodopa: toward Parkinson management, *ACS Sens.* 4 (2019) 2196–2204, <https://doi.org/10.1021/acssensors.9b01127>.
- [15] L. Lin, H.-T. Lian, X.Y. Sun, Y.-M. Yu, A L-dopa electrochemical sensor based on graphene doped molecularly imprinted chitosan film, *Anal. Methods* 7 (2015) 1387–1394, <https://doi.org/10.1039/C4AY02524E>.
- [16] S.A. Zaidi, Development of molecular imprinted polymers based strategies for the detection of dopamine, *Sensor. Actuator. B Chem.* 265 (2018) 488–497, <https://doi.org/10.1021/am5078478>.
- [17] C.C. Harley, A.D. Rooney, C.B. Breslin, The selective detection of dopamine at a polypyrrole film doped with sulfonated β -cyclodextrins, *Sensor. Actuator. B Chem.* 150 (2010) 498–504, <https://doi.org/10.1007/s12678-017-0402-x>.
- [18] L. Zhang, L. Ning, S. Li, H. Pang, Z. Zhang, H. Ma, H. Yan, Selective electrochemical detection of dopamine in the presence of uric acid and ascorbic acid based on a composite film modified electrode, *RSC Adv.* 6 (2016) 66468–66476, <https://doi.org/10.1007/s12678-017-0402-x>, <https://doi.org/10.1039/c6ra25244e>.
- [19] S. Hannah, M. Al-Hatmi, L. Gray, D.K. Corrigan, Low-cost, thin film, mass-manufacturable carbon electrodes for the detection of the neurotransmitter dopamine, *Bioelectrochemistry* 133 (2020), 107480, <https://doi.org/10.1016/j.bioelechem.2020.107480>.
- [20] M.J. Whittingham, N.J. Hurst, R.D. Crapnell, A. Garcia-Miranda Ferrari, E. Blanco, T.J. Davies, C.E. Banks, Electrochemical improvements can be realised via shortening the length of screen-printed electrochemical platforms, *Anal. Chem.* 93 (2021) 16481–16488, <https://doi.org/10.1021/acs.analchem.1c03601>.
- [21] J.P. Metters, E.P. Randviir, C.E. Banks, Screen-printed back-to-back electrochemical sensors, *Analyst* 139 (2014) 5339–5349, <https://doi.org/10.1039/C4AN01501K>.
- [22] S. Casadio, J.W. Lowdon, K. Betlem, J.T. Ueta, C.W. Foster, T.J. Cleij, B. van Grinsven, O.B. Sutcliffe, C.E. Banks, M. Peeters, Development of a novel flexible polymer-based biosensor platform for the thermal detection of noradrenaline in aqueous solutions, *Chem. Eng. J.* 315 (2017) 459–468, <https://doi.org/10.1016/j.cej.2017.01.050>.

- [23] M. Peeters, B. van Grinsven, C.W. Foster, T.J. Cleij, C.E. Banks, Introducing thermal wave transport analysis (TWTa): a thermal detection for dopamine detection by screen-printed electrodes functionalised with molecularly imprinted polymer (MIP) particles, *Molecules* 21 (2016) 552, <https://doi.org/10.3390/molecules21050552>.
- [24] T. Cowen, K. Karim, S. Piletsky, Computational approaches in the design of synthetic receptors, *Anal. Chim. Acta* 936 (2016) 62–74, <https://doi.org/10.1016/j.aca.2016.07.027>.
- [25] C.W. Foster, J.P. Metters, D.K. Kampouris, C.E. Banks, Ultraflexible screen-printed graphitic electroanalytical sensing platforms, *Electroanalysis* 26 (2014) 262–274, <https://doi.org/10.1002/elan.201300563>.
- [26] E.J. Pappert, C. Buhriend, J.W. Lipton, P.M. Carvey, G.T. Stebbins, G.C. Goetz, Levodopa stability in solution: time course, environmental effects, and practical recommendations for clinical use, *Mov. Disord.* 11 (1996) 24–26, <https://doi.org/10.1002/mds.870110106>.
- [27] A. Górska, B. Bator-Paczosa, R. Piech, Highly sensitive levodopa determination by means of adsorptive stripping voltammetry on ruthenium dioxide-carbon black-nafion modified glassy carbon electrode, *Sensors* 21 (2021) 60, <https://doi.org/10.3390/s21010060>.
- [28] G. Kresse, J. Furthmüller, Efficient iterative schemes for Ab initio total-energy calculations using a plane-wave basis set, *Phys. Rev. B Condens. Matter* 54 (1996) 11169–11186, <https://doi.org/10.1103/physrevb.54.11169>.
- [29] P.E. Blöchl, Projector augmented-wave method, *Phys. Rev. B Condens. Matter* 50 (1994) 17953–17979, <https://doi.org/10.1103/physrevb.50.17953>.
- [30] J.P. Perdew, A. Ruzsinszky, G.I. Csonka, O.A. Vydrov, G.E. Scuseria, L. A. Constantin, X. Zhou, K. Burke, Restoring the density-gradient expansion for exchange in solids and surfaces, *Phys. Rev. Lett.* 100 (2008), 136406, <https://doi.org/10.1103/PhysRevLett.100.136406>.
- [31] S. Grimme, J. Antony, S. Ehrlich, S.A. Krieg, Consistent and accurate *Ab Initio* parametrization of density functional dispersion correction (DFT-D) for the 94 elements H-Pu, *J. Chem. Phys.* 132 (2010), 154104, <https://doi.org/10.1063/1.3382344>.
- [32] M. Trchová, Z. Morávková, S. Sědčková, J. Stejskal, Spectroscopy of thin polyaniline films deposited during chemical oxidation of aniline, *Chem. Pap.* 66 (2012) 415–445, <https://doi.org/10.2478/s11696-012-0142-6>.
- [33] O. Jamieson, K. Betlem, N. Mansouri, R.D. Crapnell, F.S. Vieira, A. Hudson, C. E. Banks, C.M. Liauw, J. Gruber, M. Zubko, K.A. Whitehead, M. Peeters, Electropolymerised molecularly imprinted polymers for the heat-transfer based detection of microorganisms: a proof-of-concept study using yeast, *Therm. Sci. Eng. Prog.* 24 (2021), 100956, <https://doi.org/10.1016/j.tsep.2021.100956>.
- [34] A. García-Miranda Ferrari, C.W. Foster, P.J. Kelly, D.A.C. Brownson, C.E. Banks, Determination of the electrochemical area of screen-printed electrochemical sensing platforms, *Biosensors* 8 (2018) 53, <https://doi.org/10.3390/bios8020053>.
- [35] Y. Wang, H. Zhang, M. Chen, A strategy to differentiate dopamine and levodopa based on their cyclization reaction regulated by pH, *Anal. Chim. Acta* 1157 (2021), 338379, <https://doi.org/10.1016/j.aca.2021.338379>.
- [36] M. Hu, I. Fritsch, Application of electrochemical redox cycling: toward differentiation of dopamine and norepinephrine, *Anal. Chem.* 88 (2016) 5574–5578, <https://doi.org/10.1021/acs.analchem.6b00427>.